Quantitative Structure-Activity Relationship and Molecular Modeling Studies on a Series of Hydroxamate Analogues Acting as HDAC Inhibitors

Anubha Bajpai[1], Neeraj Agarwal[1], Vijay K. Agrawal[2], Basheerulla Shaik[2] and Satya P. Gupta[2,*]

[1]*Department of Biotechnology, Meerut Institute of Engineering and Technology (MIET), Meerut-250005, India*

[2]*Department of Applied Sciences, National Institute of Technical Teachers' Training and Research, Bhopal-462002, India*

Abstract: In this communication, a quantitative structure-activity relationship (QSAR) study has been performed on a series of trichostatin A (TSA) and suberanilo hydroxamic acid (SAHA) analogues acting as histone deacetylase (HDAC1) inhibitors to investigate their physicochemical properties that govern their activity. In this study, a significant 2D QSAR model was obtained correlating the activity of the compounds with their parachor and some indicator variables which suggested that molecules may have dispersion interaction with the receptor and that their surface tension may greatly help to this interaction. Further, the indicator parameters suggested that SO_2NH moiety present in the molecule may not be conducive to the activity, but the straight chain joining the aromatic rings with hydroxamate moiety and having ≥6 single bonds may be favorable to the activity, provided it has no substituent at any carbon. Using the model, some new compounds in the series have been predicted and docked to see their interaction with the HDAC1. All compounds have been found to have better interaction with the enzyme than TSA and SAHA, the two FDA approved HDAC inhibitors, and all the compounds obey Lipinski's rule of 5.

Keywords: Hydroxamate analogues, Histone deacetylase inhibitors, Molecular modeling, Quantitative structure-activity relationship.

1. INTRODUCTION

The enzymes, histone deacetylases (HDACs), affect the acetylation status of histones and other important cellular proteins and have been recognized as potentially useful therapeutic targets for a broad range of human disorders, such as cardiomyocyte autophagy [1,2], neurological and psychological disorders, (e.g., Schizophrenia [3] and Huntington disease [4]), and tumorigenesis and metastasis [5]. They mediate changes in nucleosome conformation and are important in the regulation of gene expression [6]. Hydroxamates are a new class of anticancer agents reported to act by selective inhibition of the histone deacetylase enzyme. HDACs have become a novel target for the discovery of drugs for the treatment of cancer and other diseases [7-12]. The number of HDAC enzyme subtypes has expanded considerably over the past few years for the development of HDAC inhibitors with improved specificity. A number of natural inhibitors, such as trichostatin A (TSA) [13], cyclic tetrapeptide trapoxin (TPX) [14], HC toxin [15] and apicidin [16], have been reported. TSA has been identified as a potent and specific HDAC inhibitor. Synthetic inhibitors, like sodium phenyl butyrate [17], sodium valprote [18], suberoylanilide hydroxamic acid (SAHA) [19], straight chain TSA and SAHA-like analogues [20-22] and oxamflatin [23], have also been reported. With the application of Quantitative Structure-Activity Relationship (QSAR) and Molecular Modeling methodologies, our aim is to discuss the mechanism of HDAC inhibition by hydroxamate analogues and to predict more potent HDAC inhibitors in the series with good ADME/T values.

2. MATERIALS AND METHODS

We performed a simple multiple linear regression (MLR) on a series of hydroxamate analogues compiled from the literature [20-22]. All the compounds are listed in Table **1** along with their HDAC inhibition activity in terms of pIC_{50}, where IC_{50} refers to molar concentration of compound leading to 50% inhibition of the enzyme. The total 56 compounds of Table **1** have been divided into two subsets: the training set comprising of 41 compounds and the test set comprising of 15 compounds. The test set compounds in the table are marked with a superscript 'b' and are given in bold. Compounds for the test set were selected keeping in view the wide variation in structures as well as in activities of compounds. The physicochemical parameter that was found to be significant in multiple linear regression (MLR) was only Parachor (PAR), which was calculated by ACD/ChemSketch (version 11.0) [24]. Several other parameters were calculated

*Address correspondence to this author at the Department of Applied Sciences, National Institute of Technical Teachers' Training and Research, Bhopal-462002, India; Tel: + 91-9368222297; Fax: + 91-755-2661996;
E-mail: spgbits@gmail.com

E-ISSN: 2308-8044/14

Table 1: Hydroxamate Analogues and their HDAC Inhibition Activities and Physicochemical Properties

No	Structure	PAR	IP_1	IP_2	IP_3	pIC_{50} [a]	Cald., Eq.1	Residual
1	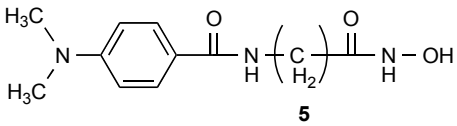 **5**	6.711	0	0	0	7.300	7.146	0.154
2	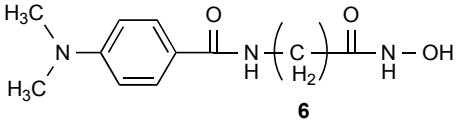 **6**	7.109	0	1	0	8.000	7.712	0.288
3	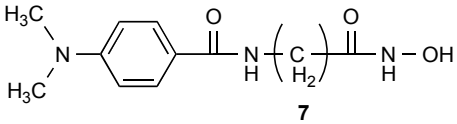 **7**	7.506	0	1	0	7.540	7.877	-0.337
4	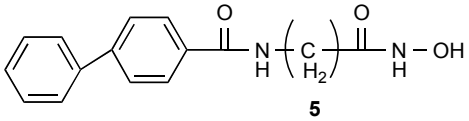 **5**	7.424	0	0	0	7.280	7.442	-0.162
5	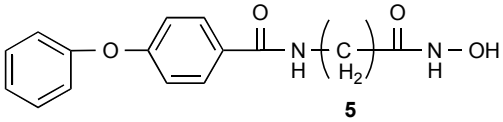 **5**	7.602	0	0	0	7.360	7.516	-0.156
6	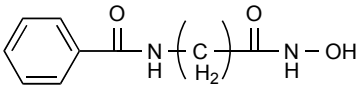 **6**	6.088	0	1	0	6.950	7.287	-0.337
7	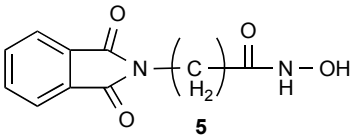 **5**	5.800	0	0	0	6.990	6.767	0.223
8	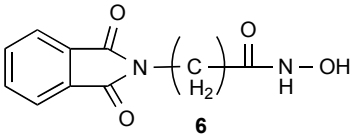 **6**	6.200	0	1	0	7.150	7.333	-0.183
9	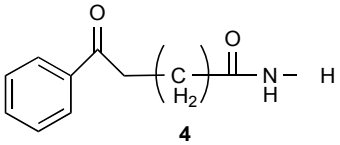 **4**	5.411	0	0	0	6.300	6.605	-0.305
10	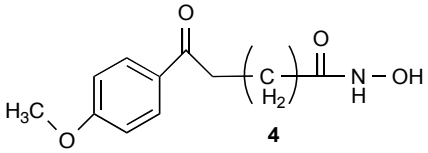 **4**	5.978	0	0	0	6.350	6.841	-0.491

(Table 1). Continued.

No	Structure	PAR	IP_1	IP_2	IP_3	pIC_{50} [a]	Cald., Eq.1	Residual
11	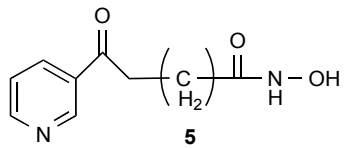 **5**	5.750	0	1	0	6.820	7.146	-0.326
12	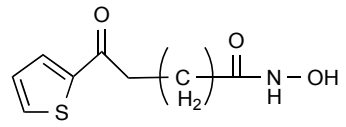 **5**	5.640	0	1	0	7.300	7.100	0.200
13	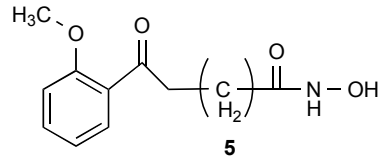 **5**	6.375	0	1	0	7.020	7.406	-0.386
14	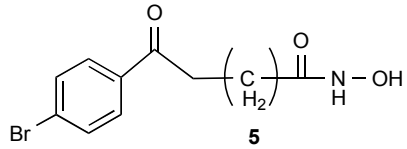 **5**	6.314	0	1	0	7.350	7.381	-0.031
15	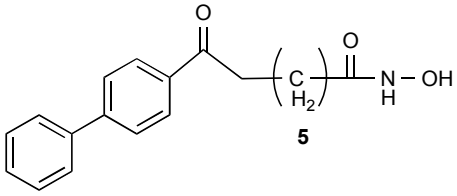 **5**	7.542	0	1	0	8.300	7.892	0.408
16	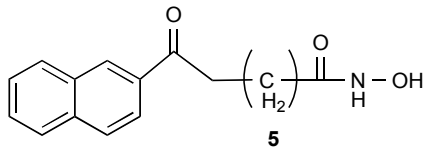 **5**	6.847	0	1	0	8.100	7.603	0.497
17	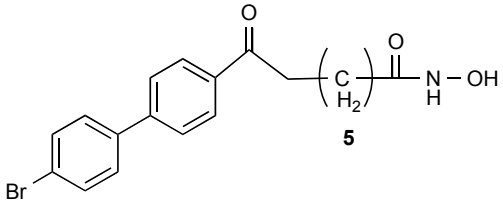 **5**	8.047	0	1	0	8.700	8.102	0.598
18	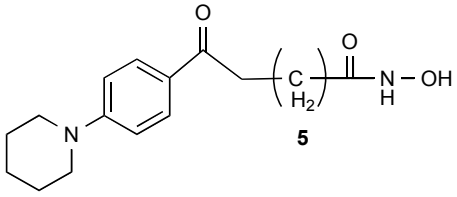 **5**	7.752	0	1	0	8.020	7.979	0.041

(Table 1). Continued.

No	Structure	PAR	IP_1	IP_2	IP_3	pIC_{50} [a]	Cald., Eq.1	Residual
19	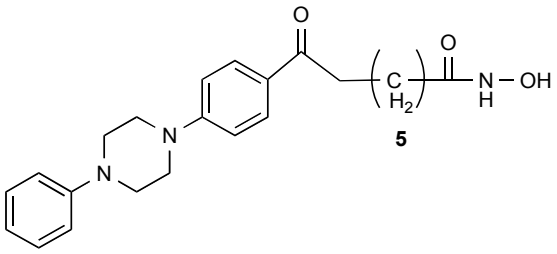 **5**	9.353	0	1	0	8.350	8.645	-0.295
20[c]	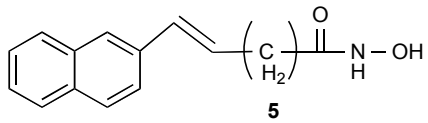 **5**	6.627	0	0	0	8.220	-	-
21	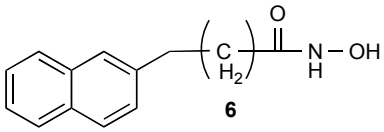 **6**	6.761	0	1	0	7.600	7.567	0.033
22	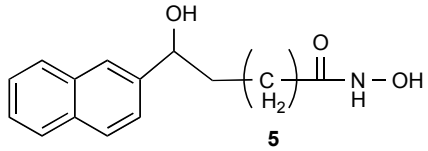 **5**	6.915	0	1	0	7.460	7.631	-0.171
23	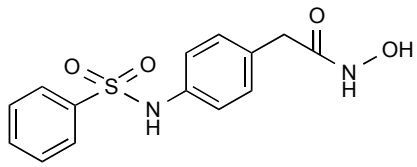	6.141	1	0	0	6.000	6.335	-0.335
24	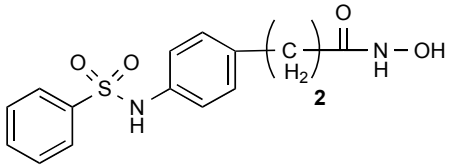 **2**	6.943	1	0	0	6.000	6.668	-0.668
25	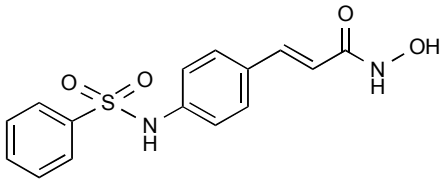	6.418	1	0	0	6.700	6.450	0.250
26	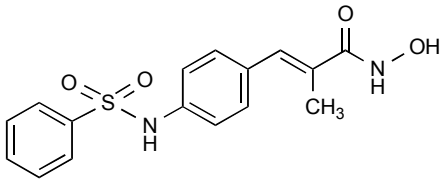	6.781	1	0	1	5.700	5.156	0.544
27	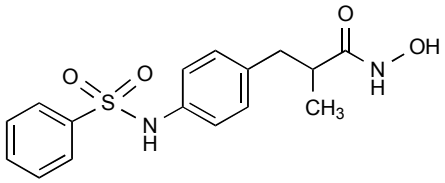	6.922	1	0	1	4.770	5.244	-0.544

(Table 1). Continued.

No	Structure	PAR	IP_1	IP_2	IP_3	pIC_{50} [a]	Cald., Eq.1	Residual
28	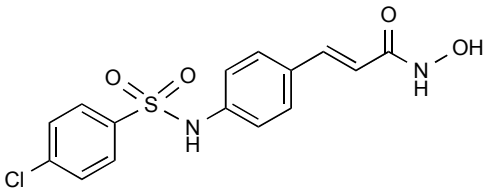	6.789	1	0	0	7.120	6.604	0.516
29	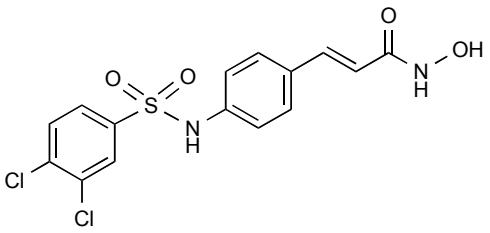	7.161	1	0	0	7.000	6.759	0.241
30	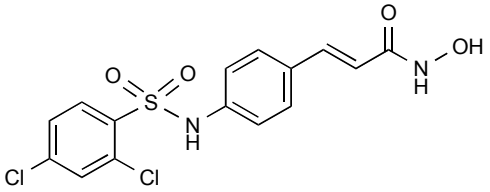	7.161	1	0	0	6.520	6.759	-0.239
31	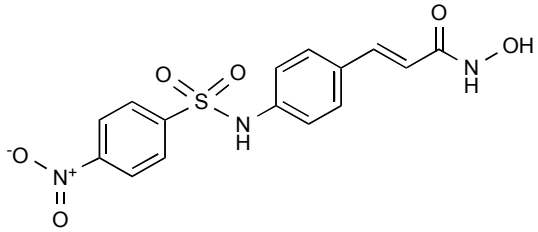	6.989	1	0	0	6.150	6.687	-0.537
32[c]	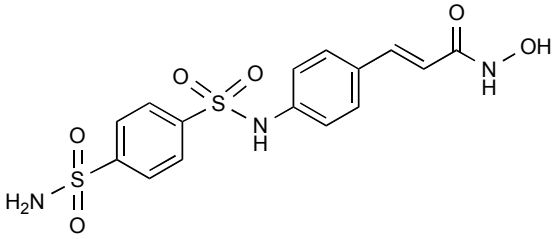	7.494	1	0	0	6.100	-	-
33	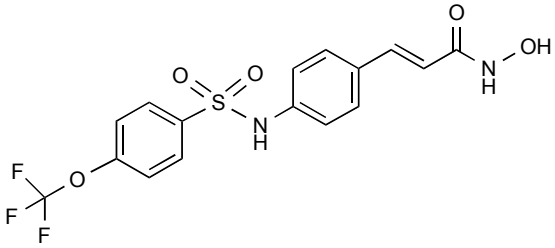	7.241	1	0	0	6.220	6.792	-0.572
34	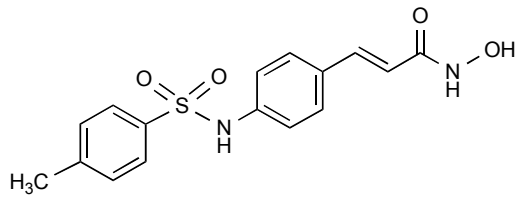	6.801	1	0	0	6.520	6.609	-0.089

(Table 1). Continued.

No	Structure	PAR	IP_1	IP_2	IP_3	pIC_{50} [a]	Cald., Eq.1	Residual
35	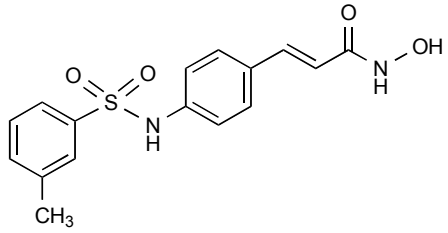	6.801	1	0	0	7.000	6.609	0.391
36	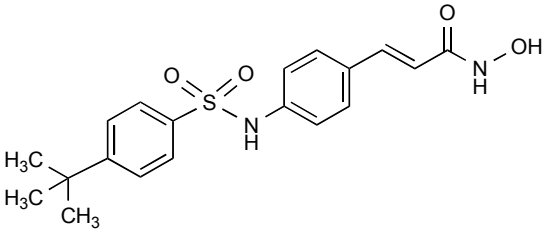	7.966	1	0	0	7.000	7.094	-0.094
37[c]	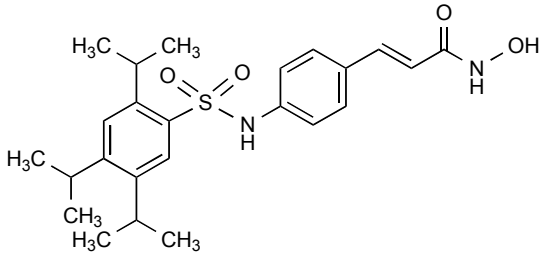	9.909	1	0	0	6.220	-	-
38	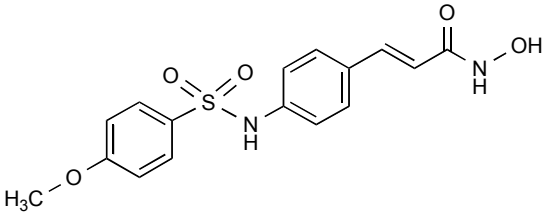	7.004	1	0	0	7.220	6.694	0.526
39	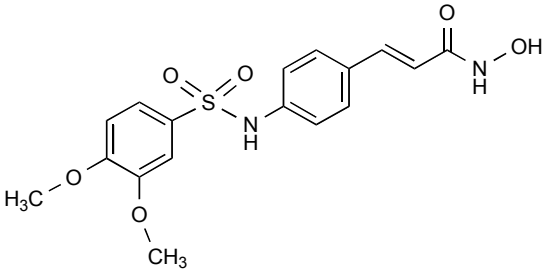	7.590	1	0	0	7.050	6.937	0.113
40[b]	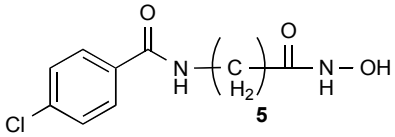	6.049	0	0	0	7.130	6.868	0.262
41[b]	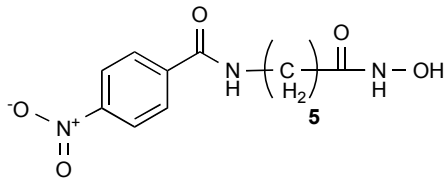	6.245	0	0	0	6.520	6.950	-0.430

(Table 1). Continued.

No	Structure	PAR	IP_1	IP_2	IP_3	pIC_{50} [a]	Cald., Eq.1	Residual
42[b]	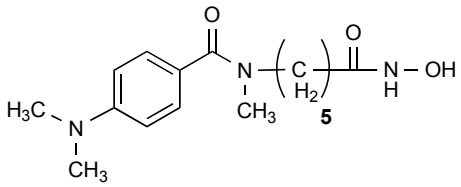	7.086	0	0	0	7.050	7.302	-0.252
43	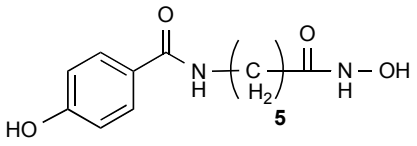	5.841	0	0	0	7.520	6.784	0.736
44[b]	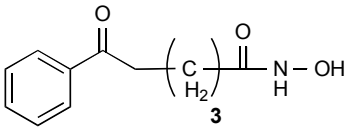	5.013	0	0	0	5.820	6.435	-0.615
45[b]	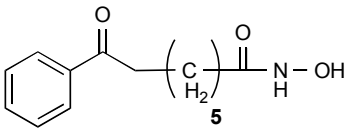	5.809	0	1	0	7.190	7.167	0.023
46[b]	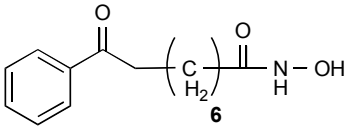	6.207	0	1	0	6.870	7.334	-0.464
47[b]	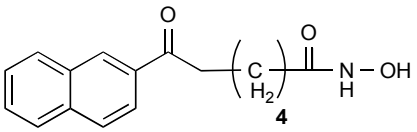	6.449	0	0	0	7.460	7.036	0.424
48[b]	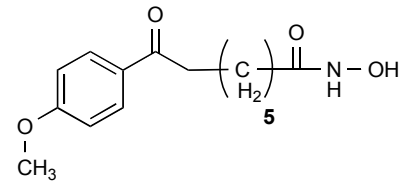	6.375	0	1	0	7.820	7.404	0.416
49[b]	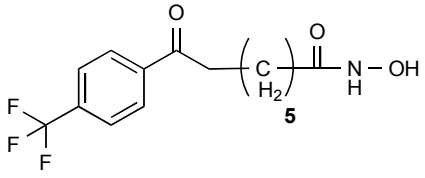	6.381	0	1	0	7.350	7.406	-0.056
50[b]	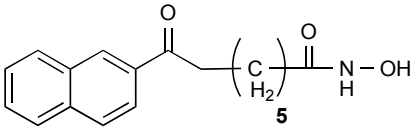	6.847	0	1	0	8.300	7.601	0.699
51[b]	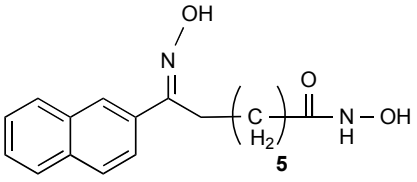	6.962	0	1	0	8.070	7.649	0.421

(Table 1). Continued.

No	Structure	PAR	IP_1	IP_2	IP_3	pIC_{50}[a]	Cald., Eq.1	Residual
52[b]	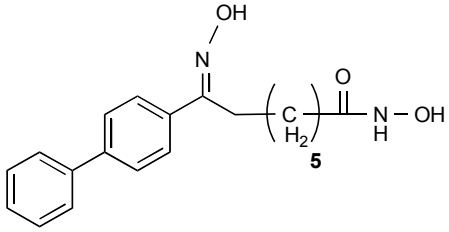 **5**	7.734	0.000	1	0	8.400	7.972	0.428
53[b]	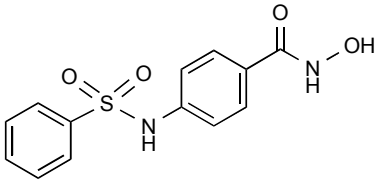	5.740	1.000	0	0	6.050	6.164	-0.114
54	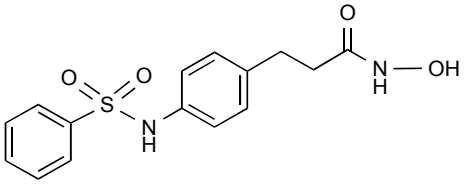	6.542	1.000	0	0	7.000	6.502	0.498
55[b]	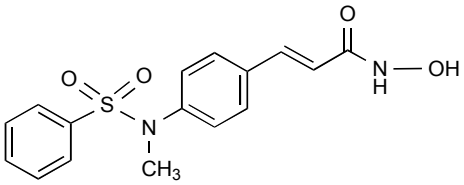	6.799	1.000	0	0	6.220	6.607	-0.387
56[b]	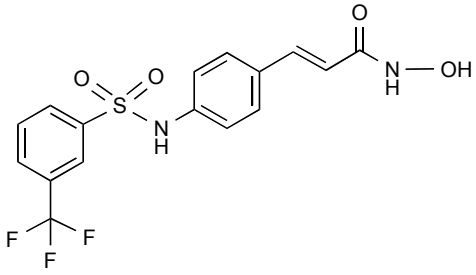	7.038	1.000	0	0	7.000	6.707	0.293

[a]Taken from refs. [20-22]. [b]Used for test set. [c]Not used in deriving Eq. (1) as they were outliers.

but found of no use. The values of this parameter for all the compounds are listed in Table **1**. In deriving QSAR model, three indicator parameters, IP_1, IP_2, and IP_3 have also been used. IP_1 has been used with a value of 1 for the presence of an -SO_2NH- moiety between two aromatic rings and IP_2 has been used for the linear chain that connects the aryl ring to the hydroxamic acid moiety. If this connecting chain contains an alkyl chain with carbon atoms ≥6, its value is 1, otherwise zero. The parameter IP_3 has been used with a value of 1 for the linear chain that has any substituent.

The sequence of HDAC1 is the same as that of HDAC2 at the active sites, and both the sequences are highly homological with HDAC8. So the homology structure of HDAC1 based on human HDAC8 in complex with TSA and SAHA (PDB entry 1T64) has been applied in this research for performing docking and to check the interactions between the predicted compounds and protein [25]. Molegro Virtual Docker software [26] (trial version) has been used for docking.

3. RESULTS AND DISCUSSION

3.1. QSAR Results

When a multiple linear regression (Hansch analysis) was performed on the compounds of the training set, it revealed the following correlation.

pIC_{50} = 0.418(±0.180)PAR − 0.575(±0.393)IP_1 + 0.399(±0.388)IP_2 −1.395(±0.619)IP_3 + 4.340(±1.190)

n = 38, r = 0.875 , r^2_{cv} = 0. 693, r^2_{pred} = 0.804, s = 0.40, $F_{4,33}$ = 26.93(3.32) (1)

In Eq. (1), n is the number of data points, r is the correlation coefficient, r^2_{cv} is the square of the cross-validated correlation coefficient obtained from leave-one-out (LOO) jackknife procedure, s is the standard deviation, F is the Fischer ratio between the variances of calculated and observed activities, and the data within the parentheses with ± sign are 95% confidence intervals. The figures within parenthesis following the F-value is the standard F-value at 99% level. The values of these statistical parameters exhibit that the correlation obtained is quite significant. The internal validity of the correlation is judged by the value of its r^2_{cv} which is calculated as:

$$r^2_{cv} = 1 - [\Sigma_i (y_{i,\ obsd} - y_{i,\ pred})^2 / \Sigma_i (y_{i,obsd} - y_{av,obsd})^2] \quad (2)$$

where $y_{i,obsd}$ and $y_{i,pred}$ are the observed and predicted (from LOO) activity values of compound i, respectively, and $y_{av,obsd}$, is the average of the observed activities of all compounds used in the correlation. The correlation is supposed to be valid if $r^2_{cv} > 0.60$. From this point of view, the correlation expressed by Eq. (1) seems to be quite valid. However, the predictive ability of any correlation equation is judged by predicting the activity of the compounds in the test set using it and calculating the value of r^2_{pred}, which is defined as:

$$r^2_{pred} = 1 - [\Sigma_i (y_{i,obsd} - y_{i,pred})^2 / \Sigma_i (y_{i,obsd} - y_{av,obsd})^2] \quad (3)$$

where $y_{i,obsd}$ and $y_{i,pred}$ refer to the observed and predicted (from eq. obtained) activity of compound i in the test set and $y_{av,obsd}$ is same as in Eq.(2). A value of r^2_{pred} equal to 0.804, signifies a good predictive ability of the correlation. The activity values predicted from this equation for the test set compounds are given (in bold) in Table **1**. A comparison shows that these predicted values are in very good agreement with the corresponding observed ones. In the training set also, the calculated values are found to be in excellent agreement with the observed ones. All these observations can be better visualized in the graphs drawn between the predicted and observed activities (Figure **1**). It is also to be noted that all the four parameters of the Eq. (1) are statistically quite significant in the correlation. Further, as shown in

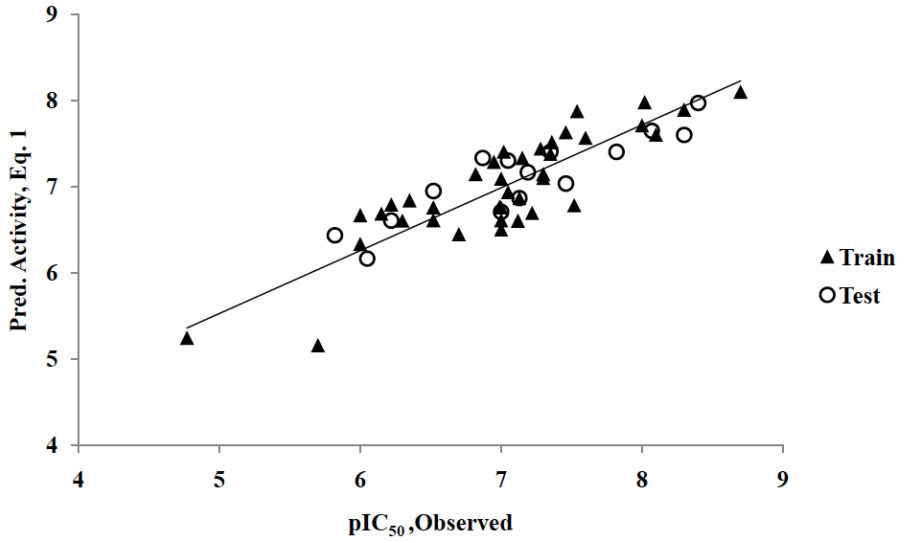

Figure 1: A plot between observed and predicted activities of training and test set compounds.

Table 2: Correlation Matrix Showing the Mutual Correlations Among the Variables Used

	PAR	IP_1	IP_2	IP_3
PAR	1.000	-0.262	-0.256	0.034
IP_1		1.000	0.696	-0.206
IP_2			1.000	-0.009
IP_3				1.000

Table 3: Some Proposed Compounds Belonging to the Series of Table 1 and their Predicted Activity

Sr. No.	Structure	PAR	IP_2	pIC_{50}
1	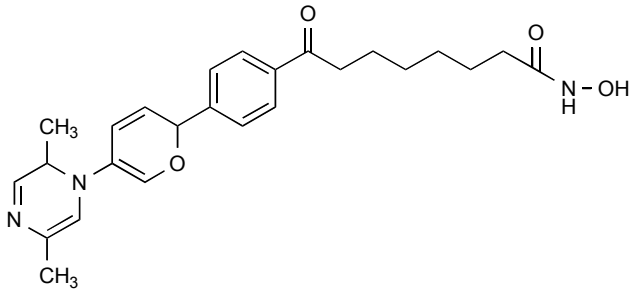	9.500	1.0	8.71
2	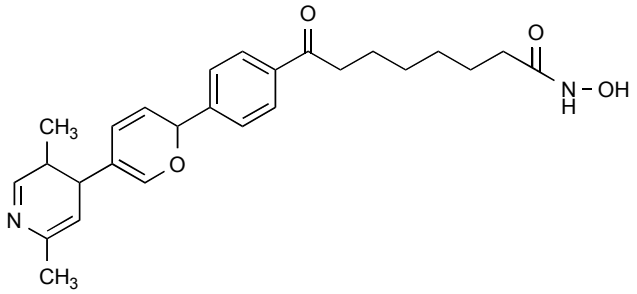	9.544	1.0	8.73
3	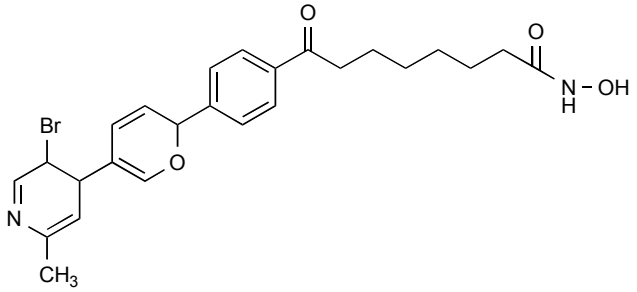	9.669	1.0	8.78
4	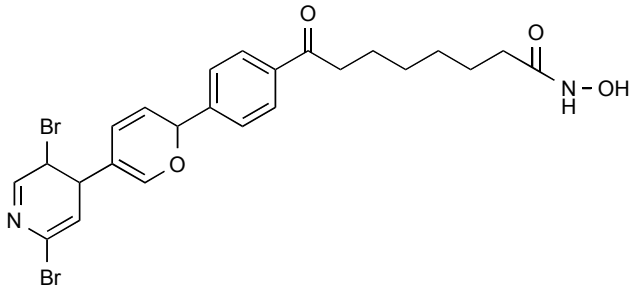	9.793	1.0	8.83
5	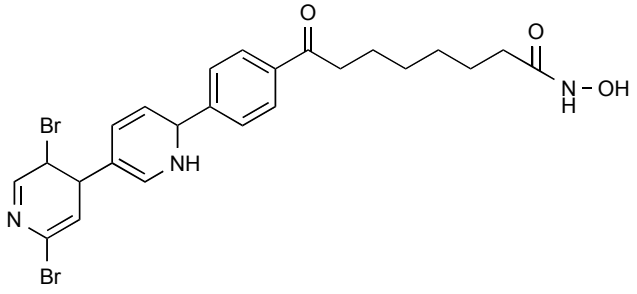	9.799	1.0	8.83

(Table 3). Continued.

Sr. No.	Structure	PAR	IP_2	pIC_{50}
6	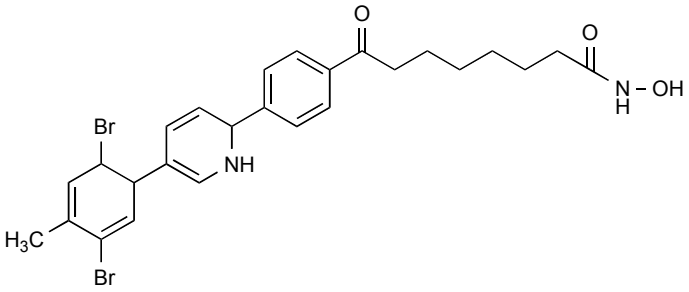	10.669	1.0	9.20
7	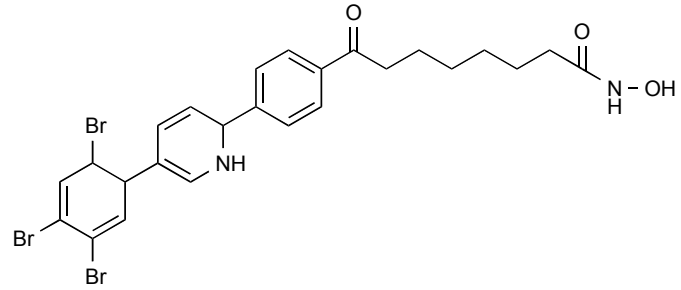	10.797	1.0	9.25
8	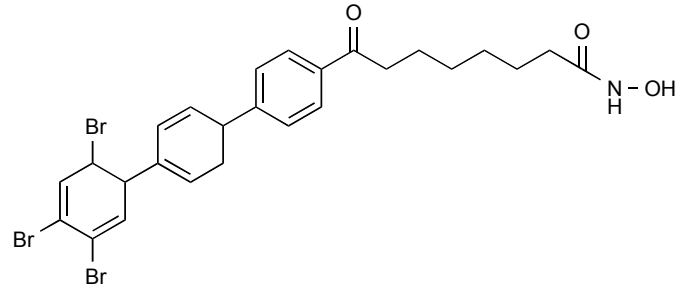	10.915	1.0	9.30
9	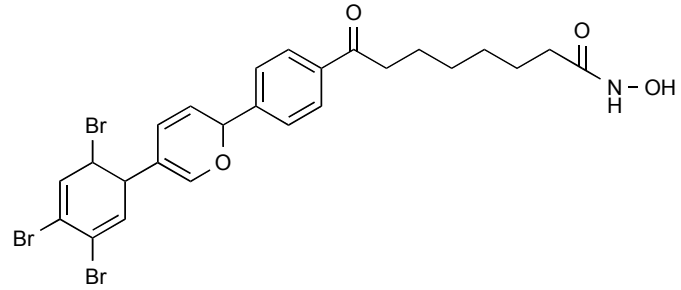	10.718	1.0	9.22
10	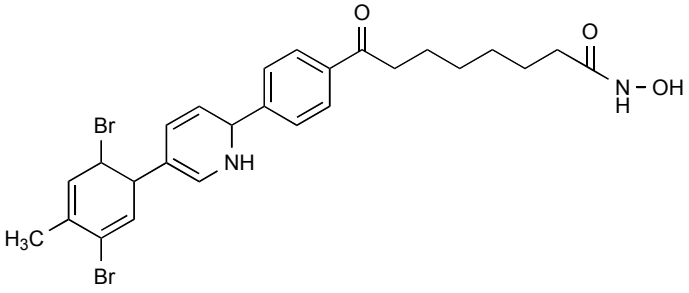	10.810	1.0	9.26

(Table 3). Continued.

Sr. No.	Structure	PAR	IP_2	pIC_{50}
11	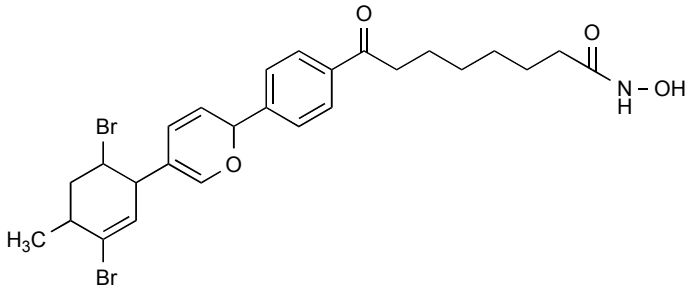	10.731	1.0	9.22
12	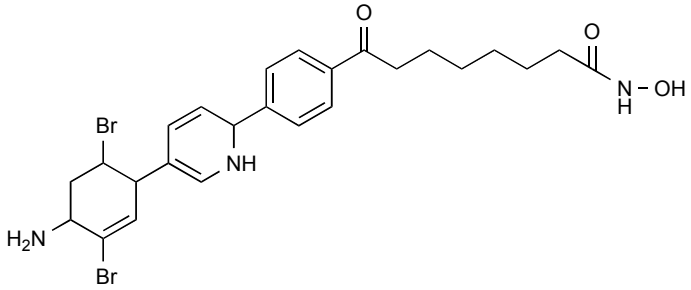	10.707	1.0	9.21
13	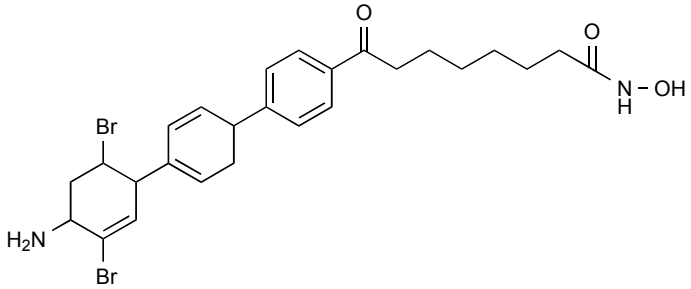	10.825	1.0	9.26
14	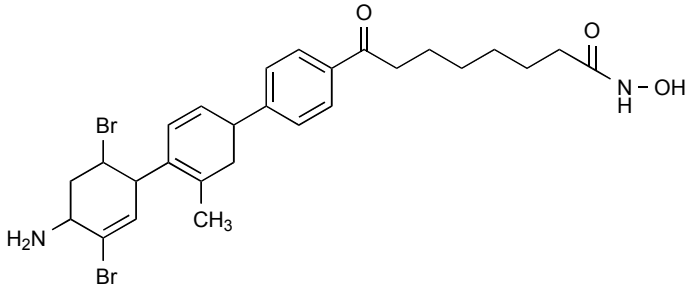	11.188	1.0	9.42
15	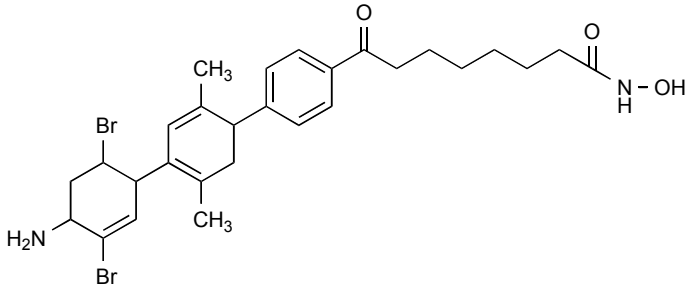	11.552	1.0	9.57

(Table 3). Continued.

Sr. No.	Structure	PAR	IP_2	pIC_{50}
16	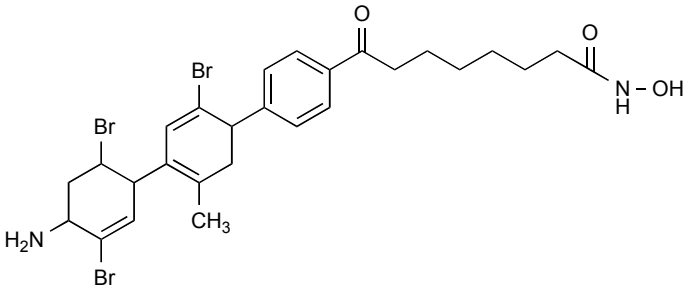	11.680	1.0	9.62
17	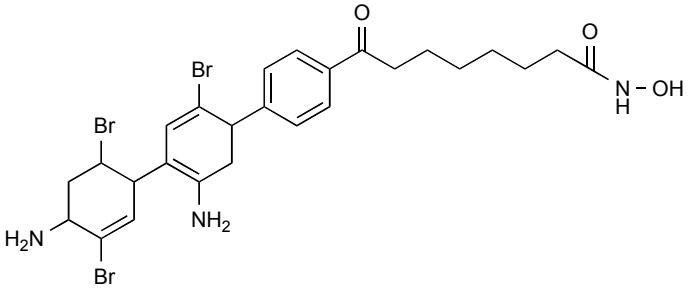	11.576	1.0	9.58

Table **2**, these variables have no significant mutual correlation. Using Eq. (1), we have predicted the activity of some new prospective compounds with high potency (Table **3**). The activities of these compounds are higher than any compound in the present series (Table **1**).

Now from Eq. (1), it can be said that the activity of compounds is basically controlled by their parachor, which is defined as

$$PAR = \gamma^{1/4} * M / d \quad (4)$$

where $\gamma^{1/4}$ is the fourth root of surface tension, M is the molar mass, and d is the density. Since M/d is equivalent to the molar volume (V_m), we can write

$$PAR = \gamma^{1/4} V_m \quad (5)$$

and thus parachor refers to the molar volume as well as the surface tension of the molecule and therefore its presence in Eq. (1) signifies that the HDAC inhibition by these compounds will be controlled by their molar volume as well as surface tension. The dependence of the inhibition activity on molar volume means that there can be dispersion interaction between the compounds and the receptor and dependence on the surface tension leads to suggest that the surface of the molecule may be highly prone to interact with the receptor.

The negative dependence of the activity on IP_1 parameter suggests that the presence of the $-SO_2NH-$ in the molecule produces a negative effect. This probably may be due to the repulsive interaction of lone pairs of electrons present on oxygen atoms with some negatively charged site of the active site in the receptor. However, the positive dependence of the activity on IP_2 parameter, that signifies the number of single bonds in the linear chain connecting to hydroxamic acid moiety, indicates that flexibility of the chain would be favorable to the activity. This flexibility of the chain might give desired conformation to the chain to have optimum interaction with the receptor. However, if there is any substituent on this chain, there can be a hindrance in obtaining the desired conformation, and thus a negative effect of such chain is indicated by the negative coefficient of the third indicator variable IP_3.

3.2. Docking Results

Molecular docking is a computational technique for exploration of the possible binding modes of a substrate or inhibitor in a given enzyme or receptor to give the optimal interactions [27]. To perform a docking, the first requirement is to have 3D structure of the receptor or protein of interest which can be determined by X-ray crystallography or NMR spectroscopy. This protein structure and a 3D database of potential ligands serve as input to a docking

program. The success of a docking program depends on two components, viz., the search algorithm and the scoring function.

Docking Simulations

Molegro Virtual Docker (MVD) was used for flexible ligand docking wherein the software makes use of differential evolution algorithm [28]. Fast and accurate identification of potential binding modes during the search process is made by the use of predicted cavities. The scoring function makes use of piecewise linear potential (PLP) [29]. The scoring function takes into account hydrogen bonding terms along with their directionality, ligand-protein interaction energy, and intramolecular interaction energy of the ligand. For enhanced docking accuracy, the highest ranked poses are yet again reranked [30].

Table 4: Docking Results of Predicated Molecules with Reference to FDA Approved Molecule

Compd	Total Interaction Energy[a]	H-Bond Energy[a]	No. of Hydrogen bonds	H-bonds	H-bonds Length (Å)
1	-218.170	-2.520	3	O(16)-Lys(289) O(16)-Gln(293) N(15)-Lys(289)	2.76 3.47 3.22
2	-207.067	-7.273	4	O(16)-Gln(549) N(15)-Gln(549) O(16)-Glu(704) O(16)-Leu(313)	3.21 3.45 3.00 3.07
3	-203.625	-2.898	3	N(15)-Lys(275) O(16)-Lys(275) N(27)-Leu(313)	3.02 2.62 3.54
4	-199.716	-5.756	3	N(33)-Lys(311) H(46)-Val(47) N(15)-Ala(48)	2.63 2.81 3.25
5	-193.745	-4.831	4	O(16)-Lys(311) O(16)-Leu(327) N(15)-Lys(311) N(32)-Leu(278)	3.23 3.28 2.85 3.13
6	-191.252	-3.758	2	O(16)-Val(61) N(15)-Ala(62)	2.68 3.16
7	-188.464	-3.032	2	O(16)-Val(61) N(15)-Ala(62)	2.83 3.27
8	-185.401	-2.500	1	O(23)-Ser(21)	2.85
9	-184.645	-4.809	3	O(16)-Lys(325) O(16)-Leu(327) N(15)-Lys(325)	3.17 3.22 2.82
10	-184.618	-3.673	2	O(16)-Val(61) N(15)-Ala(62)	2.72 3.19
11	-184.241	-4.283	2	O(16) –Lys(325) O(16)-Leu(327)	3.13 3.33
12	-182.347	-0.852	2	H(44)-Val(61) N(15)-Ala(62)	2.39 3.28
13	-177.123	0.000	0	0	0
14	-172.457	-2.500	1	O(16)-Ser(21)	2.76
15	-171.865	-2.500	1	O(16)-Val(61)	3.09
16	-168.303	-2.500	1	O(16)-Val(61)	2.92
17	-156.338	-2.500	1	O(16)-Val(61)	3.09
SAHA	-122.737	-4.341	2	N(6)-Pro(59) O(17)-Ser(21)	2.92 3.23
TSA	-116.297	-5.000	2	H(35)-Gln(80) O(10)-Tyr(241)	2.85 3.00

[a]In kJ/mol.

Validation of Docking Method

The scoring function MolDock Grid with 0.30 Å resolution along with an algorithm MolDock optimizer was used for docking. The following parameters: number of runs = 10, population size = 50, and max iterations = 2000, termination scheme = variance based were fixed. All the compounds were docked in the protein molecule (PDB id 1T64) using Molegro Virtual Docker. The docked results are cited in Table **4** along with the docked results of well-known two HDAC inhibitors, SAHA and TSA. The results show that all predicted compounds have better total interaction energy and total hydrogen-bond energy than FDA approved molecules. The docking of Compd **2**, one of the predicted compounds that have the highest number of H-bonds (Table **4**), is shown in Figures **2** and **3**, where the former shows the H-bond interactions and the latter the possible hydrophobic interactions. It can be seen that while Figure **2** shows that compound may have strong H-bond interactions with the enzyme, Figure **3** shows that compound may have no hydrophobic interaction with the enzyme, as no part of the compound appears to be in strong hydrophobic zone (shown by red). Thus, all predicted compounds seem to have good future and can be synthesized. The Lipinski's parameters of these compounds were also evaluated which are shown in Table **5**. This table shows that all compounds fulfill Lipinski's conditions, according to which potential drugs are less likely to face any problem of absorption and permeability if they fulfill four of the five conditions, namely their molecular weight (MW) is not more than 500, logP is not more than 5, number of H-bond donors (HDs) is not more than 5, and number of H-bond acceptors (HAs) is not more than 10.

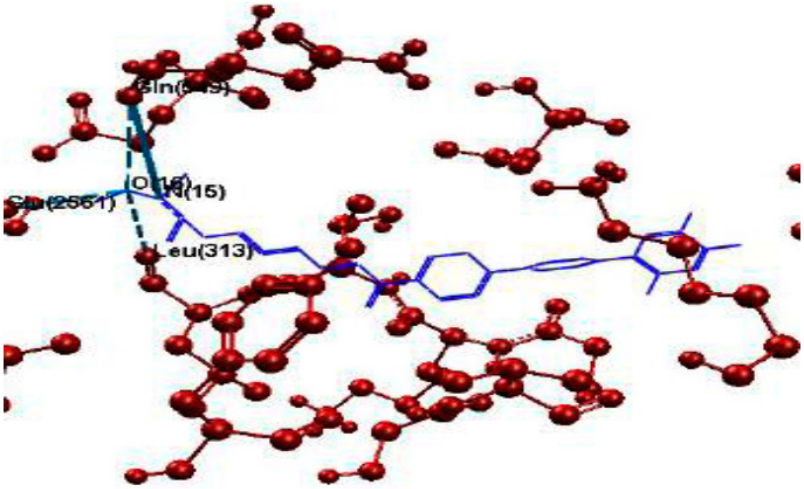

Figure 2: The model showing the H-bond interactions of Compd **2,** one of the predicted compounds that have the highest number of H-bonds (Table **4**), with HDAC1 (1T64). The enzyme is shown with red color and the compound with blue.

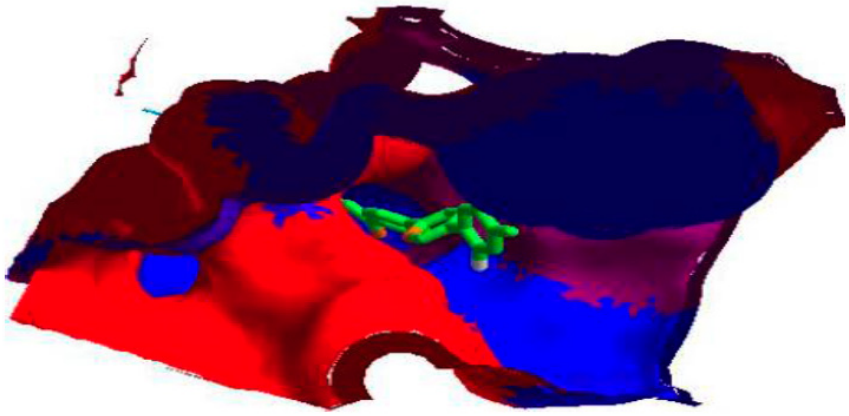

Figure 3: The model showing hydrophobic interaction of predicted Compd **2**, one of the predicted compounds that have the highest number of hydrogen bonds (Table **4**), with the enzyme (1T64). The red surface shows strong hydrophobic zone and the blue one low hydrophobic zone. The molecule does not appear to be in hydrophobic zone and thus to have any hydrophobic interaction.

Table 5: Data Related to Lipinski Rules and ADME/T Values of Predicted Compounds. Last Two Compounds are FDA Approved Compounds, they are Given for Comparison

Sr. No.	MW	HD	HA	LogP	A	D	M	E	T	pIC_{50}
1	437.531	2	6	2.52	1	5	5	6	2	8.710
2	436.543	2	5	3.25	1	5	5	7	2	8.728
3	501.413	2	5	3.45	1	5	6	7	2	8.781
4	566.282	2	5	4.34	1	6	6	8	3	8.832
5	565.297	3	5	4.02	1	7	7	8	3	8.835
6	578.336	3	4	4.75	1	7	7	9	3	9.199
7	643.205	3	4	4.91	1	7	7	9	3	9.252
8	642.217	2	3	6.03	1	6	6	9	3	9.301
9	644.190	2	4	5.23	1	7	6	9	3	9.219
10	580.352	3	4	4.92	1	7	7	9	3	9.258
11	581.337	2	4	5.24	1	7	6	9	3	9.225
12	581.340	4	5	3.30	1	6	7	7	2	9.215
13	580.352	3	4	4.42	1	7	6	8	3	9.264
14	594.378	3	4	4.66	1	7	7	9	3	9.416
15	608.405	3	4	4.91	1	7	7	9	3	9.568
16	673.275	3	4	4.99	1	7	7	9	3	9.621
17	674.263	4	5	3.28	1	6	7	7	2	9.578
SAHA	264.32	3	3	2.00	1	4	4	4	2	8.710
TSA	302.368	4	2	2.41	1	4	5	5	2	8.728

4. CONCLUSION

TSA and SAHA analogues treated here may have good activity against HDAC1 if they do not have SO_2NH moiety, as it is found to be unfavorable, probably because of lone pairs of electrons on its oxygen atoms. These lone pairs of electrons may have repulsive interaction with some negative site in the enzyme. However, long aliphatic chain with more than 6 carbon atoms and no substituent on any carbon, joining the aromatic rings with hydroxamate moiety, may be favorable. All compounds are found to have better interaction energy than TSA or SAHA, the two FDA approved compounds, with the enzyme. The docking of these compounds in the protein (PDB id 1T64) shows the involvement of compounds in H-bonding but to have no hydrophoboic interactions

REFERENSES

[1] Cao DJ, Wang ZV, Battiprolu PK, *et al.* Histone deacetylase (HDAC) inhibitors attenuate cardiac hypertrophy by suppressing autophagy. Proc Nat Acad Sci USA 2011; 108: 4123-8. http://dx.doi.org/10.1073/pnas.1015081108

[2] Wang Y, Miao X, Liu Y, *et al.* Dysregulation of histone acetyltransferases and deacetylases in cardiovascular diseases. Oxidative Med Cell Longev 2014; 641979. http://dx.doi.org/10.1155/2014/641979

[3] Tang B, Dean B, Thomas EA. Disease- and age-related changes in histone acetylation at gene promoters in psychiatric disorders. Transl Psychiatry 2011. http://dx.doi.org/10.1038/tp.2011.61

[4] Lee J, Hwang YJ, Kim KY, Kowall NW, Ryu, H. Epigenetic mechanisms of neurodegeneration in Huntington's disease. Neurotherapeutics 2013; 10: 664-76. http://dx.doi.org/10.1007/s13311-013-0206-5

[5] Glozak MA, Seto E. Histone deacetylases and cancer. Oncogene 2007; 26: 5420-32. http://dx.doi.org/10.1038/sj.onc.1210610

[6] Kourzarides T. Histone acetylase and deacetylase in cell proliferation. Curr Opin Genet 1999; 9: 40-8. http://dx.doi.org/10.1016/S0959-437X(99)80006-9

[7] Marks PA, Rifkind RA, Richon VM, Breslow R, Miller T, Kelly WK. Histone deacetylases and cancer: causes and therapies. Nat Rev Cancer 2001; 1: 194-202. http://dx.doi.org/10.1038/35106079

[8] Kelly WK, O'Connor OA, Marks PA. Histone deacetylase inhibitors: from target to clinical trials. Expert Opin Invest Drugs 2002; 11: 1695-713. http://dx.doi.org/10.1517/13543784.11.12.1695

[9] Marks PA, Richon VM, Breslow R, Rifkind RA. Histone deacetylase inhibitors as new cancer drugs. Curr Opin Oncol 2001; 13: 477-83. http://dx.doi.org/10.1097/00001622-200111000-00010

[10] Marks PA, Richon VM, Breslow R, Rifkind. Inhibitors of histone deacetylase are potentially effective anticancer agents. Clin Cancer Res 2001; 7:759-60.

[11] Phiel CJ, Zhang F, Huang EY, Guenther MG, Lazar MA, Klein PS. Histone deacetylase is a direct target of valproic acid, a potent anticonvulsant, mood stabilizer, and teratogen. J Biol Chem 2001; 76: 36734-41. http://dx.doi.org/10.1074/jbc.M101287200

[12] Meinke PT, Liberator P. Histone deacetylase: A target for antiproliferative and antiprotozoal agents, Curr Med Chem 2001; 8: 211-35. http://dx.doi.org/10.2174/0929867013373787

[13] Yoshida M, Kijima M, Akita M, Beppu T. Potent and specific inhibition of mammalian histone deacetylase both *in vivo* and *in vitro* by trichostatin. J Biol Chem 1990; 265: 17174-9.

[14] Kijima M, Yoshida M, Suguta K, Horinouchi S, Beppu T. Trapoxin, an antitumor cyclic tetrapeptide, is an irreversible inhibitor of mammalian histone deacetylase. J Biol Chem 1993; 268: 22429-35.

[15] Shute RE, Dunlap B, Rich DH. Analogues of the cytostatic and antimitogenic agents chlamydocin and HC-toxin: synthesis and biological activity of chloromethyl ketone and diazomethyl ketone functionalized cyclic tetrapeptides. J Med Chem 1987; 30: 71-8. http://dx.doi.org/10.1021/jm00384a013

[16] Han JW, Ahn SH, Wang SY, Seo GU. Apicidin, a histone deacetylase inhibitor, inhibits proliferation of tumor cells *via* induction of p21WAF1/Cip1 and gelsolin. Cancer Res 2000; 60:6068-74.

[17] Gore SD, Carducci MA. Modifying histones to tame cancer: clinical development of sodium phenylbutyrate and other histone deacetylase inhibitors. Expert Opin Invest Drugs 2000; 9: 2923-34. http://dx.doi.org/10.1517/13543784.9.12.2923

[18] Gottlecher M, Minucci S, Zhu P, *et al*. Valproic acid defines a novel class of HDAC inhibitors inducing differentiation of transformed cells. J EMBO 2001; 20: 6969-6978. http://dx.doi.org/10.1093/emboj/20.24.6969

[19] Butler LM, Agus DB, Scher HI, *et al*. Suberoylanilide hydroxamic acid, an inhibitor of histone deacetylase, suppresses the growth of prostate cancer cells *in vitro* and *in vivo*, Cancer Res 2000; 60: 5165-70.

[20] Jung M, Brosch G, Ko¨lle D, Scherf H, Gerha¨user C, Loidl P. Amide analogues of trichostatin A as inhibitors of histone deacetylase and inducers of terminal cell differentiation. J Med Chem 1999; 42: 4669-79. http://dx.doi.org/10.1021/jm991091h

[21] Remiszewski SW, Sambucetti LC, Atadja P, *et al*.Inhibitors of human histone deacetylase: synthesis and enzyme and cellular activity of straight chain hydroxamates. J Med Chem 2002; 45: 753-7.

[22] Woo SH, Frechette S, Khalil EA, *et al*. Structurally simple trichostatin A-like straight chain hydroxamates as potent histone deacetylase inhibitors. J Med Chem 2002; 45: 2877-85. http://dx.doi.org/10.1021/jm020154k

[23] Kim YB, Lee KH, Sugita K, Yoshida M, Horinouchi S. Oxamflatin is a novel antitumor compound that inhibits mammalian histone deacetylase, Oncogene 1999; 18: 2461-70. http://dx.doi.org/10.1038/sj.onc.1202564

[24] http://www.acdlabs.com

[25] Guo Y, Xiao J, Guo Z, Chu F, Cheng Y, Wu S. Exploration of a binding mode of indole amide analogues as potent histone deacetylase inhibitors and 3D-QSAR analysis, J Bio Med Chem 2005; 13: 5424-34. http://dx.doi.org/10.1016/j.bmc.2005.05.016

[26] http://www.molegro.com

[27] Gupta, SP (2011) QSAR and Molecular Modeling. Anamaya Publishers, New Delhi.

[28] Yang JM, Chen CC. A generic evolutionary method for molecular docking. Proteins 2004; 55: 288-304. http://dx.doi.org/10.1002/prot.20035

[29] Thomsen R. Flexible ligand docking using evolutionary algorithms: investigating these effects of variation operators and local search hybrids. Biosystems 2003; 72: 57-73. http://dx.doi.org/10.1016/S0303-2647(03)00135-7

[30] www.rcsb.com

Received on 24-07-2014 Accepted on 29-09-2014 Published on 05-11-2014

DOI: http://dx.doi.org/10.12970/2308-8044.2014.02.02.1